

## ORIGINAL ARTICLE

# Linking environmental heterogeneity and reproductive success at single-cell resolution

Mitja NP Remus-Emsermann<sup>1</sup> and Johan HJ Leveau<sup>1,2</sup>

<sup>1</sup>Department of Microbial Ecology, Netherlands Institute of Ecology (NIOO-KNAW), Heteren, The Netherlands and <sup>2</sup>Department of Plant Pathology, University of California, Davis, CA, USA

**Individual-based microbial ecology (IBME) is a developing field of study in need of experimental tools to quantify the individual experience and performance of microorganisms in their natural habitats. We describe here the conception and application of a single-cell bioreporter approach with broad utility in IBME. It is based on the dilution of stable green fluorescent protein (GFP) in dividing bacteria. In the absence of *de novo* synthesis, GFP fluorescence of a daughter cell approximates half of that of its mother, from which follows that the fluorescence of a progeny cell is a quantitative measure for the reproductive success of its ancestor. To test this concept, we exposed GFP-filled bacteria to different degrees of environmental heterogeneity and assessed how this affected individual cells by the analysis of GFP content in their progeny. Reporter bacteria growing in rich medium in a shaking flask showed no variation in reproductive success, confirming that life in a broth is experienced much the same from one bacterium to the next. In contrast, when reporter bacteria were released onto plant leaf surfaces, representing a microscopically heterogeneous environment, clear intrapopulation differences in reproductive success were observed. Such variation suggests that individual cells in the founding population experienced different growth-permitting conditions, resulting in unequal contributions of individual bacteria to future offspring and population sizes. Being able to assess population changes bottom-up rather than top-down, the bioreporter offers opportunities to quantify single-cell competitive and facilitative interactions, assess the role of chance events in individual survivorship and reveal causes that underlie individual-based environmental heterogeneity.**

*The ISME Journal* (2010) 4, 215–222; doi:10.1038/ismej.2009.110; published online 29 October 2009

**Subject Category:** microbe–microbe and microbe–host interactions

**Keywords:** individual-based ecology; environmental heterogeneity; bioreporter; phyllosphere; single-cell microbiology

## Introduction

Environmental heterogeneity, defined as spatial and temporal variation in the physical, chemical and biological environment, is a fundamental property of ecosystems (Scheiner and Willig, 2008). At the scale of individual organisms, it affects the ability to survive, reproduce, co-exist and interact with other organisms. For plants and animals, environmental impact can be assessed and quantified relatively simply at the level of individual organisms (Melbourne *et al.*, 2007). In microbial ecology, however, the effect of environmental variability on microbial activity and diversity is commonly assessed at a scale that is several orders of magnitude greater

than the dimensions of the microorganisms under study (Hellweger and Bucci, 2009). This ‘coarse-grained’ (Templeton and Rothman, 1978) approach to environmental heterogeneity suffers from the averaging effect that is typical of many population-based approaches (Brehm-Stecher and Johnson, 2004). It is increasingly being recognized that ‘fine-grained’ environmental heterogeneity, that is the one experienced by microscopic individuals at the micrometer-scale is a key factor in explaining microbial activity, diversity, distribution and evolution (Davey and Winson, 2003; Green and Bohannan, 2006; Prosser *et al.*, 2007; Davidson and Surette, 2008). However, due to the relative lack of tools to probe environments for micrometer-scale differences in physical, chemical or biological variables, little is known about the heterogeneity that individual microorganisms are exposed to and, more importantly, how this affects their activity and reproductive success.

Bioreporter technology (Leveau and Lindow, 2002; Harms *et al.*, 2006; Tecon and van der Meer,

Correspondence: JHJ Leveau, Department of Plant Pathology, University of California, One Shields Avenue, 476 Hutchison Hall, Davis, CA 95616, USA.

E-mail: jleveau@ucdavis.edu

Received 23 July 2009; revised 21 September 2009; accepted 21 September 2009; published online 29 October 2009

2006) relies on microorganisms themselves to report on local environmental conditions. Many of these bioreporters involve the conditional expression of green fluorescent protein (GFP), a reporter that can be quantified with relative ease in individual cells by fluorescence image microscopy (Jaspers *et al.*, 2001; Leveau and Lindow, 2001a) or flow cytometry (Axtell and Beattie, 2002; Maksimow *et al.*, 2002; Harms *et al.*, 2006; Roostalu *et al.*, 2008). When properly calibrated, the GFP signal becomes a measure for exposure to a particular environmental stimulus. For example, Leveau and Lindow (2001a) used a fructose-responsive promoter fused to the gene for GFP to probe the availability of this sugar to bacteria on plant leaf surfaces, also known as the phyllosphere (Leveau, 2006). Temporal and spatial variation in single-cell green fluorescence indicated substantial heterogeneity in the availability of fructose to individual leaf colonizers (Leveau and Lindow, 2001a). Such heterogeneity has also been reported for other nutrients or stimuli that leaf bacteria are exposed to, including iron (Joyner and Lindow, 2000), water (Axtell and Beattie, 2002), UV light (Gunasekera and Sundin, 2006) and phenolic compounds (Sandhu *et al.*, 2007).

While bacterial bioreporters, such as the ones described above, are useful in micrometer mapping of differences in the bacterial experience of single environmental variables, they cannot communicate how each of those variables, individually or jointly, impact the fate of bacteria in the environment under study. We therefore designed a bioreporter tool that describes micrometer-scale environmental heterogeneity in general terms, that is as a sum of all variables expressed into a single, quantifiable effect on the bacterium. The bioreporter we introduce here records environmental heterogeneity in terms of past reproductive success. In concept, it is based on the observation that upon cell division, GFP in a bacterial cell is distributed in a predictable manner between its two daughter cells (Rosenfeld *et al.*, 2006; Roostalu *et al.*, 2008): one division leaves cells approximately half as green fluorescent as their parent, two divisions one-fourth as fluorescent, and so on. Thus, the GFP content of an individual offspring cell becomes a quantifiable measure of reproductive success. This approach resembles the method that was used (Mailloux and Fuller, 2003) to estimate *in situ* doubling times for bacteria released into an aquifer after staining them with carboxy-fluorescein diacetate succinimidyl ester, a fluorescent protein stain that dilutes from the bacteria with every cell division. However, whereas these authors were interested solely in population averages of *in situ* growth, we tested our GFP-based bioreporter by exposure to microscopic conditions of low (that is, LB broth) and high (that is, the phyllosphere) environmental heterogeneity to reveal sub-population differences in the reproduction of single bacteria. The implications of our findings extend broadly to studies on other microbial habitats

dealing with the question of how individual bacteria in founder populations differ in their contribution to future population sizes.

## Materials and methods

### *Bacterial strains and culture conditions*

*Erwinia herbicola* 299R::JBA28 (pCPP39) (*Eh299R*::JBA28 (pCPP39)) (Leveau and Lindow, 2001b) carries a chromosomal mini-Tn5-Km transposon insertion that expresses stable GFP from a  $\text{LacI}^{\text{r}}$ -repressible  $P_{A1/O4/O3}$  promoter fusion to *gfpmut3*. The transposon confers resistance to kanamycin. The strain also harbors plasmid pCPP39, which confers tetracycline resistance and harbors a *lacI*<sup>r</sup> gene for control of  $P_{A1/O4/O3}$  activity, and thus GFP production by isopropyl- $\beta$ -D-thiogalactopyranoside (IPTG). Bacteria were cultivated at 28 °C on LB agar or in LB broth at 300 r.p.m. Where appropriate, IPTG, kanamycin or tetracycline were added to final concentrations of 1 mM, 50 or 15  $\mu\text{g ml}^{-1}$ , respectively. Optical densities of bacterial cultures were measured at 600 nm ( $\text{OD}_{600}$ ) in a Unico 1100 spectrophotometer (Unico, Dayton, NJ, USA).

### *GFP-loading, release and recovery of bioreporter Eh299R::JBA28 (pCPP39)*

Exponentially growing cells of *Eh299R*::JBA28 (pCPP39) were diluted 300-fold into fresh LB broth containing 1 mM IPTG and grown to mid-exponential phase. These GFP-loaded cells were used to inoculate plant leaves (see below) or LB broth. In the latter case, 25 ml of LB was inoculated with 200  $\mu\text{l}$  of GFP-loaded bacteria and incubated at 28 °C and 300 r.p.m. Samples were taken every 30 min to measure  $\text{OD}_{600}$  and to collect bacteria for fixation (see below). For plant inoculations, GFP-loaded bacteria were diluted in Milli-Q water to a final concentration of  $5 \times 10^4$  colony-forming units  $\text{ml}^{-1}$ . Leaves of 12–14-day old *Phaseolus vulgaris* plants (green snap bean, variety Blue Lake Bush 274) were inoculated by brief submersion into this bacterial suspension, shaken to dispose of excessive liquid and transferred to a closed translucent box for high-humidity incubation at 21 °C. At different time intervals, two leaves were transferred to a 50-ml Falcon tube with 20 ml 1  $\times$  PBS buffer, vortexed briefly and sonicated for 7 min. Part of the bacterial cells in the leaf washing was plated on agar for counting colony forming units, whereas the rest was collected on 0.2- $\mu\text{m}$  Durapore filters (Millipore, Amsterdam, The Netherlands), recovered by vortexing for 15 s in 1 ml 1  $\times$  PBS, and fixed (see below).

### *Fluorescence in situ hybridization, fluorescence microscopy and image cytometry*

Bacterial cells collected from LB broth or plant leaves were fixed as described previously (Leveau

and Lindow, 2001a) and stored at  $-20^{\circ}\text{C}$  in 50%  $1 \times$  PBS/50% ethanol for no longer than 2 weeks. To distinguish cells of *Eh299R::JBA28* (pCPP39) from indigenous bacteria on the bean leaves, fixed leaf washings were subjected to fluorescence *in situ* hybridization using an *Eh299R*-specific, TAMRA-labeled probe (Brandl *et al.*, 2001) at a final concentration of  $5.5 \text{ ng}\mu\text{l}^{-1}$ . LB- or leaf-exposed cells were examined with an Axio Imager.M1 (Zeiss, Oberkochen, Germany) using 470/20 nm excitation for the visualization of GFP and 546/6 nm for TAMRA. Digital images were captured at 1000-fold magnification with an AxioCam MRm camera (Zeiss) in phase contrast and through a 525/25 nm (GFP) or 575–640 nm (TAMRA) filter set. Using AxioVision 2.6 Software (Zeiss), single-cell GFP fluorescence was quantified as the mean-pixel intensity (Leveau and Lindow, 2001a), and expressed in units of Sferes (Standardized fluorescence reference), where 1 milliSferes equals one-thousandth of the average mean-pixel intensity of 1- $\mu\text{m}$  Tetraspek Fluorescent Microsphere Standards (Molecular probes, Eugene, OR, USA). Data analyses and simulations were performed in Microsoft Excel 2003 (Microsoft Corporation, Redmond, WA, USA). For computer simulations presented in Figure 3a, reproductive success was calculated for 100 cells with a green fluorescence (GF) equal to  $X/2^t$ , in which X equals the Excel formula ‘=norminv(rand(),1000,250)’. Figure 3b shows the temporal changes in reproductive success of individual bacteria as a function of  $t$  from a population of 90 cells with  $\text{GF} = X$  and  $10 \cdot 2^t$  cells with  $\text{GF} = X/2^t$ . Figure 3c shows the reproductive success of 20 bacteria with  $\text{GF} = X$ ,  $20 \cdot 2^{0.125 \cdot t}$  bacteria with  $\text{GF} = X/2^{0.125 \cdot t}$ ,  $20 \cdot 2^{0.25 \cdot t}$  bacteria with  $\text{GF} = X/2^{0.25 \cdot t}$ ,  $20 \cdot 2^{0.5 \cdot t}$  bacteria with  $\text{GF} = X/2^{0.5 \cdot t}$  and  $20 \cdot 2^t$  bacteria with  $\text{GF} = X/2^t$ . Figure 3d shows the reproductive success in a population of 20 bacteria with  $\text{GF} = X$ ,  $20 \cdot 2^t$  bacteria with  $\text{GF} = X/2^t$  ( $t \leq 1$ ) or  $20 \cdot 2^1$  bacteria with  $\text{GF} = X/2^1$  ( $t > 1$ ),  $20 \cdot 2^t$  bacteria with  $\text{GF} = X/2^t$  ( $t \leq 2$ ) or  $20 \cdot 2^2$  bacteria with  $\text{GF} = X/2^2$  ( $t > 2$ ),  $20 \cdot 2^t$  bacteria with  $\text{GF} = X/2^t$  ( $t \leq 3$ ) or  $20 \cdot 2^3$  bacteria with  $\text{GF} = X/2^3$  ( $t > 3$ ) and  $20 \cdot 2^t$  bacteria with  $\text{GF} = X/2^t$ .

## Results

### GFP dilution is a quantitative measure for reproductive success

A previously formulated mathematical model of GFP expression in bacteria (Leveau and Lindow, 2001b) predicts that in the absence of *de novo* synthesis, GFP dilutes from dividing cells at a rate equal to growth rate  $\mu$ . We verified this prediction here using *Eh299R::JBA28* (pCPP39), which accumulates stable GFP in the presence of the synthetic inducer IPTG. Upon transfer of IPTG-induced GFP-loaded cells to broth that lacked IPTG, GFP fluorescence declined exponentially and at a rate that was not significantly different from  $\mu$  (Figure 1).

No such decrease in fluorescence was observed when GFP-loaded cells were transferred to sterile Milli-Q water (data not shown), confirming that GFP is extremely stable in this strain and that its dilution from cells depends on division.

From Figure 1, it follows that the average number of cell divisions since  $t = 0$  can be calculated from the GFP fluorescence at times  $t$  ( $\text{GFP}_t$ ) and  $t = 0$  ( $\text{GFP}_0$ ) as  ${}^2\log(\text{GFP}_0/\text{GFP}_t)$ . This value is essentially a measure of reproductive success; in simple terms, it means that the dimmer a cell is, the more successful its ancestor was in producing offspring. Figure 2a shows that in an exponentially growing bacterial population in LB broth, the reproductive success of individual cells (which for any individual cell was calculated as  ${}^2\log[\text{average cell's GFP fluorescence at } t = 0 \text{ divided by single cell's fluorescence at time } t]$ ) was normally distributed. The parallel lines signify that over time, all cells contributed with equal success to the population increase (Figure 2a). This observation is consistent with the assumption that a shaking LB culture represents a homogeneous environment.

A very different result was obtained when GFP-loaded cells of *Eh299R::JBA28* (pCPP39) were released onto leaf surfaces of bean plants. In this environment (which is devoid of IPTG, see below), progeny bacteria showed considerably more variation in reproductive success compared with those in LB (Figure 2b), with clear deviation from the parallel lines observed in Figure 2a. This suggests that some immigrant cells to the leaves contributed more progeny to the population than others.

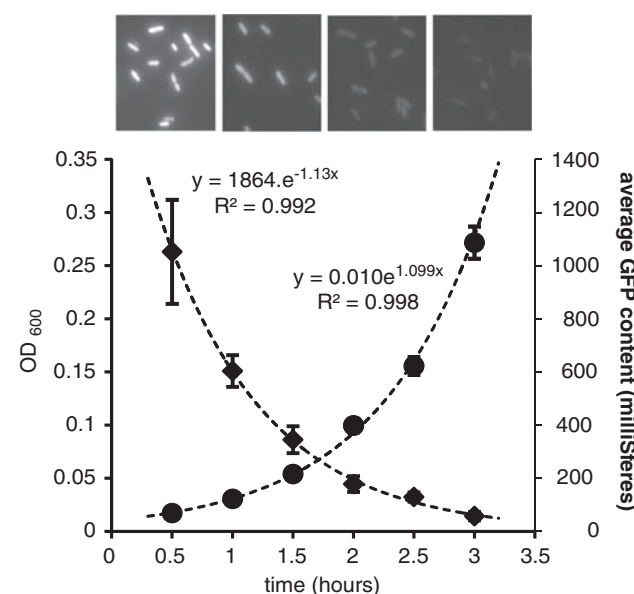


**Figure 1** Optical density (●) and average single-cell green fluorescence protein (GFP) content (◆) of GFP-loaded *Eh299R::JBA28*(pCPP39) growing in a shaken liquid LB broth. Fitted lines indicate a growth rate of  $1.10 \text{ h}^{-1}$  and a GFP dilution rate of  $1.13 \text{ h}^{-1}$ . Also shown are representative fluorescence microscopy images of cells at  $t = 0, 1, 2$  and  $3 \text{ h}$  (left to right).

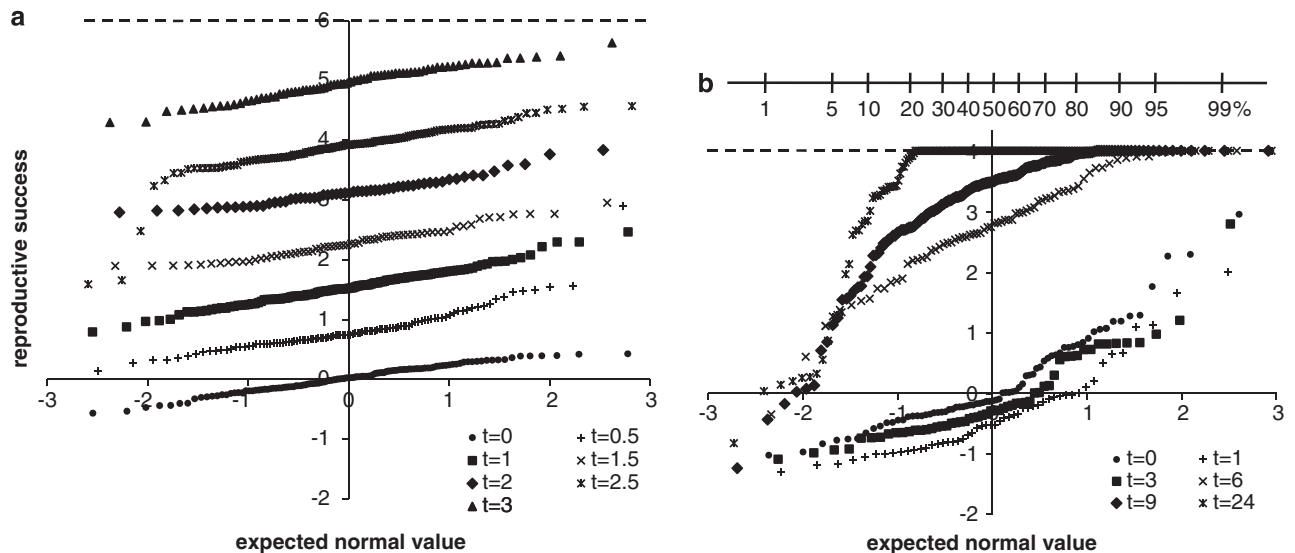


**Figure 2** Normal probability plot showing the reproductive success of *Eh299R::JBA28* (pCPP39) under low (a) and high (b) environmental heterogeneity. (a) Bioreporter cells growing in a shaken LB culture flask. (b) Bioreporter cells growing on plant leaf surfaces. Cells were sampled at the indicated times and examined for green fluorescence protein (GFP) content as described in Materials and methods. Each data point represents an individual cell, for which the reproductive success was calculated as  ${}^2\log[\text{average cell's GFP fluorescence at } t=0, \text{ divided by single cell's fluorescence at time } t]$ . The broken line represents the limit of detection, which is determined by the lowest detectable level of GFP fluorescence in a single cell. To distinguish bioreporter cells from indigenous bacteria recovered from the leaf surface, we needed to include a fluorescence *in situ* hybridization (FISH) step (see Material and methods), which reduced the GFP fluorescence of the average cell by fourfold compared with unhybridized cells and changed the detection limit of reproductive success from 6 to 4 divisions. At the top of panel b is shown a scale that translates expected normal value (on the x axis) into cumulative percentage.

In a control experiment, we introduced an uninduced culture of *Eh299R::JBA28* (pCPP39) onto leaf surfaces. Analysis of bacteria recovered from leaves after 24 h revealed that they had remained non-fluorescent, confirming that (1) the leaf surface was devoid of IPTG or other compounds that might induce *de novo* synthesis of GFP and (2) loss of plasmid pCPP39 (which would lead to constitutive expression of GFP) did not occur during the course of the experiment.

#### Modeling of GFP dilution in individual cells

To facilitate interpretation of the experimental data from the leaf surface, we ran four simple simulations (see Materials and methods) to examine the effects of different scenarios of environmental heterogeneity on the shape of reproductive success distributions. In the first scenario, all cells experienced the same conditions for maximal growth, much like the experiment in LB broth. This resulted in normal distributions of reproductive success (Figure 3a), as expected and as observed experimentally (Figure 2a). In a second scenario, the starter population was split into two sub-populations, one of which, representing an arbitrary 10% of the cells, had a maximum reproductive success rate, whereas 90% were unsuccessful at producing offspring (Figure 3b). In the other two simulations, the starter population was divided into five equal sub-populations, each of which produced progeny at different rates (Figure 3c) or produced progeny at the same

maximum rate but ceased doing so at different times during the course of the simulation (Figure 3d).

Comparison of the simulated distribution curves to the experimental ones suggests that it is unlikely that the leaf surface consists of only two types of locales: one that fully supports bacterial growth and another that does not. Based on Figure 3b, this would have resulted in the clear separation of two sub-populations in the distribution curves. Instead, it seems more likely that leaf locales represent a sliding scale in their ability to support growth of initial colonizers. Figures 3c and d show that patterns of increased heterogeneity can be simulated by assuming sub-populations that differ in their ability to reproduce, either through being offered less than favorable growth conditions or by being offered less time or resources to reproduce. Which one of these scenarios applies to the leaf surface, or whether it is a combination of the two, cannot be easily resolved by comparison of experimental to simulated data. However, both simulations prove the point that heterogeneity in reproductive success is indicative of a starter population in which cells are exposed to different growth-permitting conditions, resulting in unequal contributions to future offspring and population sizes.

#### Bacterial immigrants to the phyllosphere contribute differentially to leaf population sizes

Based on these simulations, we interpreted the experimental leaf data (Figure 2b) as follows. During

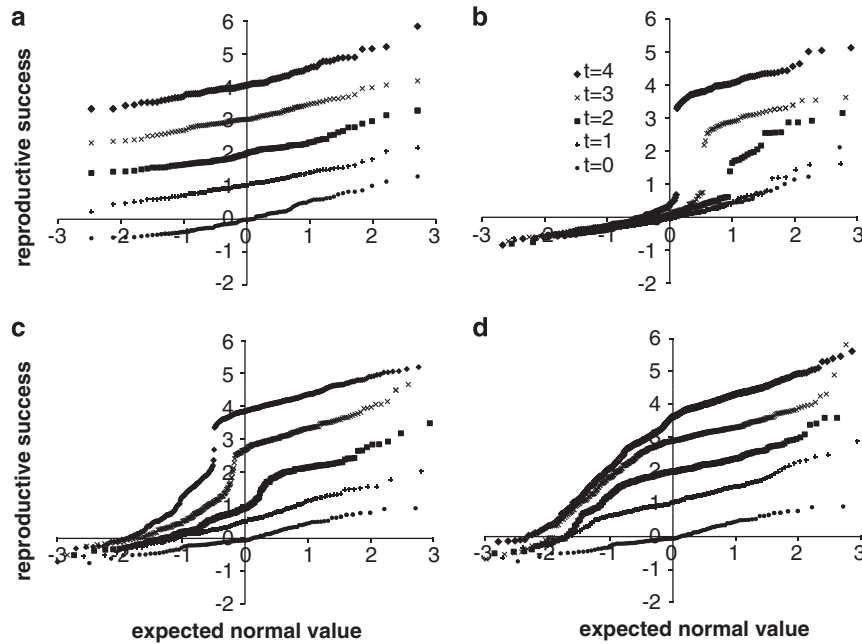


**Figure 3** Simulations of reproductive success in bacterial populations with different intrapopulation growth rates. See text for details on panels (a–d). Data points with the same shape correspond to the same single simulated sampling time. Time is expressed as generations, not in hours.

the first 3 h, GFP content did not differ significantly from  $t=0$  across the population, suggesting that the bacteria did not reproduce during that time. Six hours after inoculation, >90% cells appeared in a straight line more or less parallel to the  $t=0$  distribution, but with an average reproductive success of 2.9 divisions. This suggests that during the early period of colonization, most cells encountered similar conditions, allowing them to contribute equally to an approximately  $2^{2.9}$ , that is 7.5-fold population increase. About 5% of the cells appeared brighter than expected. These might represent cells with ancestors that settled in spots unfavorable for growth. With time, the shape of the distribution curve changed (Figure 2b). At  $t=9$  h, approximately 3% of the cells had divided 0 times, 2% 1 time, 8% 2 times, 36% 3 times and 51% 4 times or more. Extrapolated to  $t=0$ , this means that 22%, 7%, 15%, 33% and 23% of the starter population contributed 3%, 2%, 8%, 36% and 51%, respectively, of the population at  $t=9$  (Figure 4). In other words, while nearly one-third of the starter cells contributed only 5% to the population size at  $t=9$ , less than one-fourth eventually contributed more than half. These data confirm that bacterial immigrants to the leaf surface contributed differently to population sizes, which is consistent with the hypothesis that the fate of individual immigrants is determined in large part by the environmental heterogeneity at the microscopic leaf level. We were unable to make estimates of relative contribution for the  $t=24$  population, as 79% of the cells had divided beyond the limit of GFP detection.

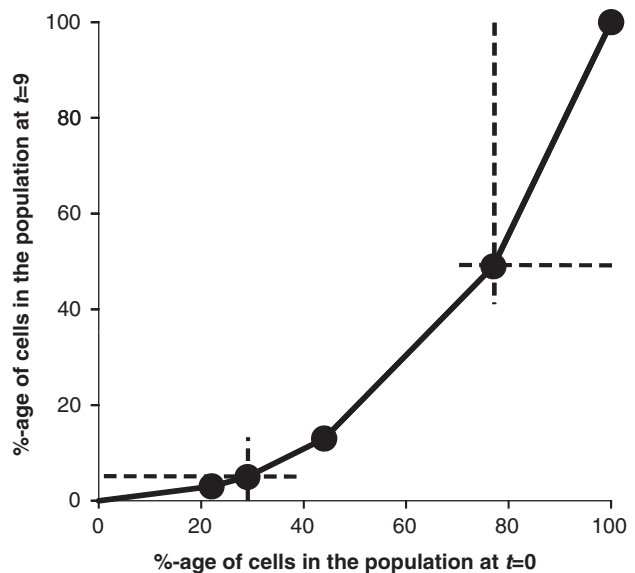


**Figure 4** Unequal contribution of bacterial founder cells to leaf population sizes. Plotted on the y axis is the cumulative percentage of cells with 0, 1, 2, 3 or  $\geq 4$  divisions 9 h after inoculation onto the leaf surface, as determined by their green fluorescence protein (GFP) content, versus on the x axis the cumulative percentage that these cells represented in the founder population at  $t=0$ . The latter was calculated by extrapolation to  $t=0$ ; for example, the 8% of bacteria that appeared to have divided twice by  $t=9$  constitute  $8/2^2$  divided by the sum of  $3/2^0$ ,  $2/2^1$ ,  $8/2^2$ ,  $36/2^3$  and  $51/2^4$  equals 15% at  $t=0$ . The convex shape of the line indicates uneven contribution of individual founder cells to the total population size. For example, the subpopulations at the bottom-left and the top-right of the graph represent similarly sized fractions (29% and 23%, respectively) of the founder population, but differ 10-fold (5% and 51%, respectively) in their contribution to the population at  $t=9$ .

### Estimating population changes from single-cell data

Figure 5a shows the changes in bacterial population sizes on the leaves, as determined by plate counting. The growth curve follows a pattern that is typical for this type of plant inoculation experiment, including a short lag, a phase of rapid growth and a level-off to apparent carrying capacity. It is interesting to note that this pattern can be reproduced quite well using only the single-cell data. From  $N = N_0 \cdot e^{\mu t}$  (in which  $N$  is the number of cells at time  $t$ , and  $N_0$  is the number of cells at  $t = 0$ ) and  $GFP = GFP_0 \cdot e^{-\mu t}$  (in which  $GFP$  is the average single-cell GFP content at time  $t$ , and  $GFP_0$  is the average single-cell GFP content at  $t = 0$ ),  $\mu$  and  $t$  can be eliminated to reveal that  $N/N_0$  equals  $GFP_0/GFP$ . In other words, a plot of  $GFP_0/GFP$  as a function of time produces in essence a growth curve, which is indeed confirmed for our data in Figure 5b. The underestimation of growth by the single-cell data at  $t = 9$  and  $t = 24$  is likely because of the fact that the reproductive success of a portion of the cells was undervalued because their GFP content was below the limit of fluorescence detection. Combined, Figures 4 and 5 demonstrate that our GFP bioreporter allows the assessment of population growth at the individual as well as population level.

## Discussion

The experimental data we present here demonstrate the utility of the ‘reproductive success’ concept by offering new insight into bacterial phyllosphere colonization. The heterogeneity that we observed in the ability of individual immigrants to produce offspring on the leaf surface is a novel observation. It corroborates findings of others who have documented leaf-based heterogeneity in environmental stimuli (Joyner and Lindow, 2000; Leveau and Lindow, 2001a; Axtell and Beattie, 2002; Gunasekera and Sundin, 2006), each of which is likely to affect reproduction. Together, these data support the

hypothesis that local conditions are the key determinants of the abundance and dynamics of microbes on plant leaf surfaces (Woody *et al.*, 2007).

We noted striking similarities in the interpretation of leaf colonization patterns based on our bioreporter data and those from a previously described bioreporter that is also *E. herbicola*-based but measures fructose availability (Leveau and Lindow, 2001a). In both cases, bacterial cells appeared to experience a period of adaptation immediately after immigration to the leaf surface. In the experiment presented here, this period of adaptation was accompanied by a reduction in cell size (data not shown), which concentrated the GFP fluorescence signal in the bacteria, resulting in brighter green fluorescent cells and lower apparent values for reproductive success (Figure 2b). This initial period of adaptation was followed by a period of reproduction for nearly all immigrants. The fructose bioreporter revealed that bacteria differ substantially in their subsequent access to fructose, causing them to deplete their resources and cease dividing at different times during colonization. This parallels our observation here of unequal contributions to the population size (Figure 2b). These lines of evidence suggest that heterogeneity in fructose availability at the micrometer scale has an important role in the reproductive success of individual bacterial immigrants to the leaf surface.

Our observations of intra-population variability in the reproduction of bacteria on leaf surfaces are compatible with current theories of aggregative behavior of bacteria in the phyllosphere. Various studies (Morris *et al.*, 1998; Monier and Lindow, 2004) have shown that many or most bacteria on naturally or experimentally inoculated leaves occur not as isolated cells but in aggregates. Aggregation has been explained to result from the differential survival and growth of solitary and aggregated cells (Monier and Lindow, 2003). In the case of *Pseudomonas syringae* (Monier and Lindow, 2004), the frequency distribution of the number of cells per

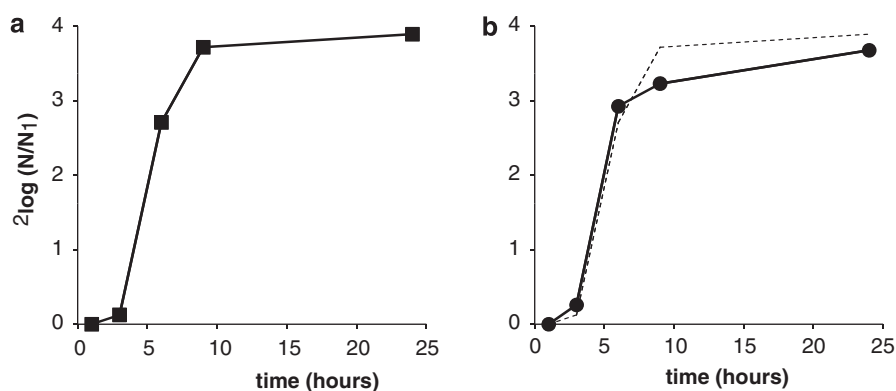


**Figure 5** Bacterial growth on leaf surfaces as determined by plate counts of colony forming units (a) and by estimation from green fluorescence protein (GFP) content of individual cells (b). The construction of panel b is described in more detail in the text. Owing to the unavailability of comparable colony counts for leaves at  $t = 0$ , both graphs compare population sizes relative to time point  $t = 1$  h. The stippled line in panel b serves as a reference representing the shape of the curve in panel a.

aggregate was found to be right-hand skewed, representing a sliding scale from many aggregates with few bacteria to few aggregates with many bacteria. Assuming that each aggregate arose from a single founder cell, a right-hand skewed distribution of aggregate sizes would indeed translate into a curved distribution of reproductive success, much like we observed for *E. herbicola* cells on leaves after prolonged exposure to the leaf surface (Figures 2b and 5b).

A limitation of our bioreporter is the inability to interpret reproductive success for cells in which GFP is diluted beyond the limit of detection. In our most optimal setup, this corresponded to six doublings, or 64 progeny cells from a single ancestor. This is sufficient for studies that are relatively short-term, involve bacteria with low rates of reproduction, or habitats with low or intermediate degrees of environmental heterogeneity. The need for fluorescence *in situ* hybridization to distinguish bioreporters from indigenous cells made it impossible to follow bacterial reproduction beyond four divisions. In future versions of the bioreporter, this may be solved by complementation of the bioreporter with a GFP-compatible, constitutively expressed fluorescent protein, for example red fluorescent mCherry (Shaner *et al.*, 2004). An additional advantage is the prospect of *in situ* observation of the bioreporter independent of its GFP fluorescence. Thus, one can start to interpret ancestral success of individual bacteria in the context of their location in the micrometer landscape.

Despite this room for improvement, the bioreporter in its current form offers several unique opportunities and advantages. One of its strengths is that reproductive success is recorded in the GFP content of each cell, which is a major advantage for studies that allow only intermittent observation or that necessitate destructive sampling of the environment, as most experiments in microbial ecology do. Another plus of the reproductive success bioreporter is that it offers microbial ecologists low-ambiguity output. Most GFP bioreporters are promoter-based, and although promoters can be quite specific in response to the environmental variable under investigation, their activity can be modulated in unpredictable ways by other input from the environment (Leveau and Lindow, 2001b). Such ambiguity makes promoter-based bioreporters susceptible to misinterpretation, particularly in the absence of proper controls (Leveau and Lindow, 2001b). The reproductive-success bioreporter is promoter-independent in that it is solely based on dilution of previously synthesized GFP from the cell by division, hence with the minimal likelihood of misinterpretation of GFP output. Such types of bioreporters are expected to have the broadest and most reliable utility in microbial ecology. Another major advantage of our bioreporter is its compatibility with many other single-cell interrogation techniques (Davey and Kell, 1996; Brehm-Stecher

and Johnson, 2004) with the ultimate goal to link reproductive success at single-cell resolution to specific bacterial behaviors or environmental experiences, and to identify the sources of heterogeneity and their impacts on bacterial individuals and on population structure and activity.

## Acknowledgements

We thank Maria Marco for useful comments on the paper and Steve Lindow for his support in the conception phase of the project. Funding was provided by the Netherlands Organisation of Scientific Research (NWO) in the form of a personal VIDI grant to JHJL. This is NIOO-KNAW publication 4626.

## References

- Axtell CA, Beattie GA. (2002). Construction and characterization of a *proU-gfp* transcriptional fusion that measures water availability in a microbial habitat. *Appl Environ Microbiol* **68**: 4604–4612.
- Brandl MT, Quinones B, Lindow SE. (2001). Heterogeneous transcription of an indoleacetic acid biosynthetic gene in *Erwinia herbicola* on plant surfaces. *Proc Nat Acad Sci USA* **98**: 3454–3459.
- Brehm-Stecher BF, Johnson EA. (2004). Single-cell microbiology: tools, technologies, and applications. *Microbiol Mol Biol Rev* **68**: 538–559.
- Davey HM, Kell DB. (1996). Flow cytometry and cell sorting of heterogeneous microbial populations: the importance of single-cell analyses. *Microbiol Rev* **60**: 641–696.
- Davey HM, Winson MK. (2003). Using flow cytometry to quantify microbial heterogeneity. *Curr Issues Mol Biol* **5**: 9–15.
- Davidson CJ, Surette MG. (2008). Individuality in bacteria. *Annu Rev Genet* **42**: 253–268.
- Green J, Bohannan BJM. (2006). Spatial scaling of microbial biodiversity. *Trends Ecol Evol* **21**: 501–507.
- Gunasekera TS, Sundin GW. (2006). Role of nucleotide excision repair and photoreactivation in the solar UVB radiation survival of *Pseudomonas syringae* pv. *syringae* B728a. *J Appl Microbiol* **100**: 1073–1083.
- Harms H, Wells MC, van der Meer JR. (2006). Whole-cell living biosensors—are they ready for environmental application? *Appl Microbiol Biotechnol* **70**: 273–280.
- Hellweger FL, Bucci V. (2009). A bunch of tiny individuals—individual-based modeling for microbes. *Ecol Modell* **220**: 8–22.
- Jaspers MCM, Meier C, Zehnder AJB, Harms H, van der Meer JR. (2001). Measuring mass transfer processes of octane with the help of an *alkS-alkB::gfp*-tagged *Escherichia coli*. *Environ Microbiol* **3**: 512–524.
- Joyner DC, Lindow SE. (2000). Heterogeneity of iron bioavailability on plants assessed with a whole-cell GFP-based bacterial biosensor. *Microbiology* **146**: 2435–2445.
- Leveau JHJ. (2006). Microbial communities in the phyllosphere. In: Riederer M and Mueller C (eds). *Biology of the Plant Cuticle*. Blackwell Publishing Ltd: Oxford, UK, pp 334–367.

- Leveau JHJ, Lindow SE. (2001a). Appetite of an epiphyte: quantitative monitoring of bacterial sugar consumption in the phyllosphere. *Proc Nat Acad Sci USA* **98**: 3446–3453.
- Leveau JHJ, Lindow SE. (2001b). Predictive and interpretive simulation of green fluorescent protein expression in reporter bacteria. *J Bacteriol* **183**: 6752–6762.
- Leveau JHJ, Lindow SE. (2002). Bioreporters in microbial ecology. *Curr Opin Microbiol* **5**: 259–265.
- Mailloux BJ, Fuller ME. (2003). Determination of *in situ* bacterial growth rates in aquifers and aquifer sediments. *Appl Environ Microbiol* **69**: 3798–3808.
- Maksimow M, Hakkila K, Karp M, Virta M. (2002). Simultaneous detection of bacteria expressing *gfp* and *dsred* genes with a flow cytometer. *Cytometry* **47**: 243–247.
- Melbourne BA, Cornell HV, Davies KF, Dugaw CJ, Elmendorf S, Freestone AL *et al.* (2007). Invasion in a heterogeneous world: resistance, coexistence or hostile takeover? *Ecol Lett* **10**: 77–94.
- Monier JM, Lindow SE. (2003). Differential survival of solitary and aggregated bacterial cells promotes aggregate formation on leaf surfaces. *Proc Nat Acad Sci USA* **100**: 15977–15982.
- Monier JM, Lindow SE. (2004). Frequency, size, and localization of bacterial aggregates on bean leaf surfaces. *Appl Environ Microbiol* **70**: 346–355.
- Morris CE, Monier JM, Jacques MA. (1998). A technique to quantify the population size and composition of the biofilm component in communities of bacteria in the phyllosphere. *Appl Environ Microbiol* **64**: 4789–4795.
- Prosser JI, Bohannan BJM, Curtis TP, Ellis RJ, Firestone MK, Freckleton RP *et al.* (2007). The role of ecological theory in microbial ecology. *Nature Rev Microbiol* **5**: 384–392.
- Roostalu J, Joers A, Luidalepp H, Kaldalu N, Tenson T. (2008). Cell division in *Escherichia coli* cultures monitored at single cell resolution. *BMC Microbiol* **8**: 68.
- Rosenfeld N, Perkins TJ, Alon U, Elowitz MB, Swain PS. (2006). A fluctuation method to quantify *in vivo* fluorescence data. *Biophys J* **91**: 759–766.
- Sandhu A, Halverson LJ, Beattie GA. (2007). Bacterial degradation of airborne phenol in the phyllosphere. *Environ Microbiol* **9**: 383–392.
- Scheiner S, Willig M. (2008). A general theory of ecology. *Theor Ecol* **1**: 21–28.
- Shaner NC, Campbell RE, Steinbach PA, Giepmans BNG, Palmer AE, Tsien RY. (2004). Improved monomeric red, orange and yellow fluorescent proteins derived from *Discosoma sp.* red fluorescent protein. *Nat Biotechnol* **22**: 1567–1572.
- Tecon R, van der Meer JR. (2006). Information from single-cell bacterial biosensors: what is it good for? *Curr Opin Biotechnol* **17**: 4–10.
- Templeton AR, Rothman ED. (1978). Evolution in fine-grained environments: 1. environmental runs and evolution of homeostasis. *Theor Popul Biol* **13**: 340–355.
- Woody ST, Ives AR, Nordheim EV, Andrews JH. (2007). Dispersal, density dependence, and population dynamics of a fungal microbe on leaf surfaces. *Ecology* **88**: 1513–1524.